Calculations of Electrical Breakdown in Air at Near-Atmospheric Pressure

A. L. WARD

Harry Diamond Laboratories, Washington, D. C.

A computer program based on the Townsend avalanche model, but explicitly including space charge, has been used to calculate electrical breakdown in air at near-atmospheric pressure. A good fit to Bandel's experimental temporal-current-growth curves may be obtained by using a secondary ionization coefficient that includes 10% ion and 90% photon portions. Only a poorer fit could be obtained when using a 100% photon effect, with either a fixed photon delay independent of overvoltage or a constant reduced electron mobility to simulate an attachment-detachment process. The same agreement and disagreement, respectively, were obtained by comparison of the results of calculations with the breakdown-time-versus-overvoltage measurements of Fisher and Bederson. The effect of variations of the number of initiating electrons from the cathode and of the approach voltage is detailed. The calculations indicate that a luminous front propagates from the anode to the cathode at a velocity of up to $\sim 3 \times 10^7$ cm/sec in the final calculable stages of breakdown.

I. INTRODUCTION

THERE are two basic models used in explaining the electrical breakdown in gases at high pressures.[1] The two models are popularly known as the Townsend avalanche model and the streamer model. For some time it had been generally accepted that the avalanche model was valid at low gas pressures and for low overvoltages and that the photoionization streamer developed in the contrary cases. Fisher and Bederson (FB)[2] attempted to pinpoint the region of transition between the two modes of breakdown by measuring formative time lags as a function of overvoltages, but without success. They proposed that the avalanche mechanism caused a buildup of space charge, which set the stage for the final streamer breakdown. Bandel[3] measured the temporal buildup of current during the formative time lag and found theory and experiment in disagreement. He suggested a delayed-photon mechanism as a possible explanation of the failure of the theory. Dutton, Haydon, and Llewellyn-Jones[4] showed that FB's data were consistent with a secondary-cathode mechanism which includes a 90% contribution by photon impact (γ_p) and a 10% contribution by positive ion impact (γ_i). Dutton *et al.* used asymptotic solutions which neglected initial conditions and space-charge distortion in the final buildup. Miyoshi[5] made calculations corresponding to Bandel's and FB's experimental conditions, which included appropriate initial conditions, but accounted for space charge only after the current was calculated using constant ionization coefficients and mobilities. He made detailed calculations for various ratios of γ_i to γ_p for a 1% overvoltage, but gave no indication as to the ratio required for

agreement with measurements. Recently Köhrmann[6] has been able to get good agreement with Bandel's measurements by assuming no ion contribution to the secondary coefficient. He used instead a lower electron mobility to simulate the effect of attachment, and later detachment, of electrons during their transit across the gap.

The present calculations are the first to include space-charge effects directly in conjunction with the continuity equations. It is the purpose of this paper to show that, when space-charge effects are included, the avalanche model is adequate for explaining the entire breakdown transition in air near atmospheric pressures.

II. THE MODEL FORMULATION

The formulation used for digital computation has been outlined previously[7,8]; further details are now included.

The model used is one-dimensional, and thus is exact only when the cross section of the discharge is constant and has a diameter large compared with the gap distance d.

The continuity equations relating the variation of charge densities $\rho_\pm = n_\pm e$ and current densities $j_\pm$ with time t in an ionizing gas are

$$\partial \rho_\pm / \partial t = \alpha(x,t) j_-(x,t) \pm \partial j_\pm / \partial x, \qquad (1)$$

where α is Townsend's first ionization coefficient and the distance x is measured from the cathode. The particle velocities and currents are considered positive when the positive ions move toward the cathode and the electrons move toward the anode. The electric-field intensity E is considered positive when directed from the anode to the cathode. Since diffusion is neglected in the formulation, the current densities are given

[1] For a comprehensive review, see I. S. Marshak, Usp. Fiz. Nauk **71**, 631 (1960) [English transl.: Soviet Phys.—Usp. **3**, 624 (1961)].

[2] L. H. Fisher and B. Bederson, Phys. Rev. **81**, 109 (1951). Hereafter designated as FB.

[3] H. W. Bandel, Phys. Rev. **95**, 1117 (1954).

[4] J. Dutton, S. C. Haydon, and Llewellyn Jones, Brit. J. Appl. Phys. **4**, 170 (1953).

[5] Yasunori Miyoshi, Phys. Rev. **117**, 355 (1960).

[6] W. Köhrmann, Z. Naturforsch. **19a**, 245 (1964); also personal communication.

[7] A. L. Ward, *Proceedings of the Fifth International Conference on Ionization Phenomena in Gases*, edited by H. Maecker (North-Holland Publishing Company, Amsterdam, 1961), Vol. 2, p. 1595.

[8] W. Börsch-Supan and H. Oser, J. Res. Natl. Bur. Std. **67B**, 41 (1963).

by

$$j_{\pm}=\rho_{\pm}v_{\pm}=\rho_{\pm}\mu_{\pm}E(x,t). \qquad (2)$$

However, it has been shown that the difference equations used for numerical computation yield an almost perfect analog for particle diffusion.[9]

A constant electron mobility is assumed, but the ion mobility is field-dependent according to the following scheme:

$$v_{+}=\mu_{+}(1-C_1Ep^{-1})E/p \qquad E/p\leq W_1$$
$$v_{+}=k_{+}(1-D_1E^{-3/2}p^{3/2})E^{1/2}/p^{1/2} \quad E/p\geq W_1, \qquad (3)$$

where p is the pressure and C_1, D_1, and W_1 are empirical constants. Poisson's equation, from which the field distortion due to space charge is determined, is

$$\partial E/\partial x=(\rho_{-}-\rho_{+})/\epsilon_0, \qquad (4)$$

where ϵ_0 is the permittivity of free space. (Note that E and x are oppositely directed.)

To compute the variation of α with field in the molecular gases, the traditional Townsend equation

$$\alpha=Ap\,\exp-(Bp/E) \qquad (5)$$

has been used. The empirical constants A and B may take on different values above and below an arbitrary value of E/p.

Two boundary conditions are required on the current densities and one on the field. The ion current density at the anode is set at zero: $j_{+}(d,t)=0$. The electron current density at the cathode is the sum of three parts: (1) a constant externally produced photocurrent J_0, (2) a current arising from positive-ion bombardment of the cathode and equal to $\gamma_i j_{+}(0,t)$, where γ_i is known as Townsend's ion secondary coefficient, here assumed constant, and (3) a variable photoelectric current arising from discharge-produced photons. Two options are available for the last-mentioned term. First, the photons can be considered to eject electrons from the cathode with no delay other than the finite time step used in the difference equations. Second, the simple delayed-photon model introduced by Menes[10] may be used. The electron current density from the cathode in this model is

$$\Gamma=\gamma_p\tau^{-1}\int_0^d\int_{-\infty}^t \sigma(x,t')j_{-}(x,t')\exp\left[\frac{-(t-t')}{\tau}\right]dt'dx, \qquad (6)$$

where σ is the excitation coefficient, defined analogously to α and having the same functional field variation; γ_p is the photon secondary coefficient, a constant that must include a geometrical factor as well as any photon absorption; and τ is the decay time of the excited state emitting the pertinent photon. This formulation may also simulate other delay mechanisms, such as the imprisonment of radiation, with less accuracy.

[9] A. L. Ward, J. Appl. Phys. 35, 469 (1964).
[10] M. Menes, Phys. Rev. 116, 481 (1959).

The boundary condition on the field is set by the external circuit. The simplest plausible circuit was chosen: a voltage supply $V(t)$ and a resistance R in series with the tube and a parallel capacitance C. The capacitance C does not include that of the gap itself, but is always necessary to account for stray or lead capacitances. The voltage $V(t)$ may be a constant, it may include a step function at $t=0$ and/or at $t=T$, or it may have a small sinusoidal component superimposed at $t=T$. The boundary condition $E(0,t)$ is then determined by[8]

$$V(t)=\int_0^d E(x,t)dx+\left[\left(C+\frac{\epsilon_0 S}{d}\right)\frac{dV}{dt}+SJ(t)\right]R, \qquad (7)$$

where S is the constant area of the discharge, $\epsilon_0 S/d$ is the gap capacitance, and

$$J(t)=J_{-}(t)+J_{+}(t)=d^{-1}\int_0^d[j_{-}(x,t)+j_{+}(x,t)]dx.$$

Calculations are made with difference equations using M intervals across the gap. The initial electron and ion distributions across the gap must be supplied as two sets of $M+1$ numbers, giving densities in cm^{-3} units. These numbers, together with the tube voltage at $t=0$, completely determine the initial field distribution.

The time step used in the calculations is limited by stability considerations. First, no particle may travel further than one distance step $\Delta x=d/M$ in the time Δt.[8] An input parameter F determines Δt through

$$\Delta t=F\Delta x/\max v_{-}(x,t), \qquad (8)$$

where $F<1$ ensures stability. There is a computer option to neglect electron transport when $\gamma_i>\gamma_p$, but this option was not used in any of the calculations included in this paper. It has been shown that the electron diffusion coefficient D_0, in the absence of space charge, is given by[9]

$$D_0/\mu_{-}=(1-F)V/2M, \qquad (9)$$

where V is the tube voltage. The ratio of the diffusion current to the conduction current of the electrons is given in the constant field case by

$$\frac{D_0\Delta n/\Delta x}{n\mu_{-}E}=\frac{D_0}{\mu_{-}}\frac{1}{\Delta V}\frac{\Delta n}{n}=\frac{(1-F)}{2}\{\exp[\alpha(\Delta x)]-1\}, \qquad (10)$$

where Δn and $\Delta V=V/M$ are the change of electron density and voltage, respectively, in the distance $\Delta x=d/M$.

The second limitation on the time step choice is imposed by the external circuit. The time step must be less than double the time constant of the external circuit.[8] This is seldom a limitation, except when electron transport is neglected. An auxiliary program to calculate equilibrium current-growth constants for

various values of M and in the absence of space charge is used to check the main program. It also yields the breakdown voltage as a function of M, the number of distance intervals across the gap. Some results of these comparisons will be mentioned later.

Computer output includes $V(t)$, $J_+(t)$, $J_-(t)$, $J(t)$, Δt, and $\Gamma(t)$ at desired time intervals, or at desired $J(t)$ values. Also printed out at the same times are $E(x,t)$, $n_+(x,t)$, $n_-(x,t)$, $j_+(x,t)$, and $j_-(x,t)$ for desired multiples of Δx.

III. PARAMETERS FOR CALCULATIONS

All calculations were made for a gap distance of 1 cm and a pressure of 722 Torr, the latter being one value used in Bandel's experiments.[3] Since FB[2] found little variation of breakdown times as a function of overvoltage between atmospheric pressure and about 200 Torr, it was not considered necessary to study the effect of small pressure changes. FB's results are given in Fig. 1. A straight line with a slope of -1.0 is drawn through their data. This line indicates an overvoltage of 0.03% for a 100 μsec breakdown time, the maximum time measurable with FB's apparatus. If their measured overvoltages are increased by 0.03%, Fig. 1 shows that the breakdown time varies inversely with overvoltage to the limit of their measurements.

The constants A and B of Eq. (5) were chosen as 8 cm^{-1} $Torr^{-1}$ and 247 V cm^{-1} $Torr^{-1}$ for all values of E/p. These constants give a reasonable fit to published data[11] of Townsend coefficients in air for $35 < E/p < 200$. The total secondary coefficient γ was chosen to be 1.5×10^{-5}, as used by Bandel[3] in his calculations. These parameters yield a breakdown voltage $V_{BO} = 28.516$ kV, compared with Bandel's average value of about 28.8 kV. The auxiliary program (mentioned earlier) shows that for 20 intervals across the gap, $V_{BO}(M=20) = 27.425$ kV for 100% γ_p and 27.441 kV for 80% γ_p. The error in V_{BO} varies approximately inversely with M. Calculations of overvoltage as cited below used these values of V_{BO} for the appropriate cases.

Unless stated otherwise, an electron mobility of $4.0 \times 10^5/p$ cm^2/V-sec was used. The constants which determine the positive ion mobility through Eq. (3) are $\mu_+ p = 2 \times 10^3$ Torr cm^2/V-sec, $C_1 = 4 \times 10^{-3}$ Torr-cm/V, $k_1 p^{1/2} = 1.25 \times 10^4$ $Torr^{1/2}$ $cm^{3/2}/V^{1/2}$-sec and $W_1 = 50$ V/cm-Torr. D_1 is calculated internally by the computer. All mobility values are essentially those used by Bandel,[3] where the literature is cited. Lacking better knowledge, the excitation coefficient was set equal to the ionization coefficient for all calculations. This was done because the photons responsible for the cathode effect are believed to be the higher energy ones. This assumption has been universally used in discussing γ_p to γ_i ratios. The factor F in Eqs. (8) and (9) was
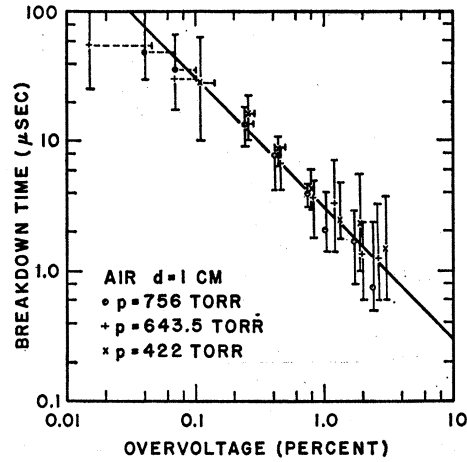
FIG. 1. Measured breakdown times as a function of overvoltage (o.v.) by Fisher and Bederson.[2] This figure was drawn from tabulated data in the unpublished thesis of Dr. Bederson. Points show average values, usually of 10 determinations; limit bars give maximum and minimum values. Solid line is drawn for reference in later figures. Horizontal limit bars give a 0.03% o.v. correction for 100-μsec breakdown time, the limit of measurements.[2]

set at 0.8, giving an electron diffusion energy of ~ 140 eV. This unreasonably high value, dictated mainly by the small M value required to keep computation times reasonable, is thought not to cause appreciable errors since concentration gradients were usually small. From Eq. (10) we find, for $F=0.8$, that the ratio of the diffusion to the conduction current of electrons is 0.1 $\Delta n/n$ or $\sim 8\%$ for $M=20$ and $\sim 3\%$ for $M=40$.

Other parameters, including the approach voltage $V(0)$, applied voltage V_a, area S, photocurrent J_0, resistance R, capacitance C, and the ratio of γ_p to γ, were changed from run to run. Unless specified otherwise, the same initial $(t=0)$ distribution of ions and electrons across the gap was used in all calculations, approximately that obtaining with an approach voltage of 2 kV below V_{BO}. For $V(0)=26.5$ kV, the initial current density $J(0)$ equals 1.9×10^{-10} A/cm^2. Also, the photon delay time τ was set equal to zero unless otherwise specified.

IV. RESULTS AND DISCUSSION

Typical calculated current growth curves are shown in Fig. 2. The solid curves are those measured by Bandel.[3] The long-dashed curves were computed assuming 90% γ_p and 10% γ_i, while the short-dashed curve resulted from assuming 80% γ_p and 20% γ_i.[12] The two curves with individual points were obtained assuming 100% γ_p, with a delayed process photon (circles) or a reduced electron mobility (crosses). Since Bandel did not measure the overvoltage used in his measurements, only the general shape of the families of curves

[11] F. H. Sanders, Phys. Rev. 41, 667 (1932); 44, 1020 (1933). K. Masch, Arch. Elektrotech. 26, 589 (1932). F. Llewellyn Jones, in *Handbuch der Physik*, edited by S. Flügge (Springer-Verlag, Berlin, 1965), Vol. 22, p. 31.

[12] No inference should be made that a better fit for the longer formative time lags is obtained using 20% γ_i rather than 10% γ_i. It is felt that the expense of an additional long calculation is not warranted at this time.
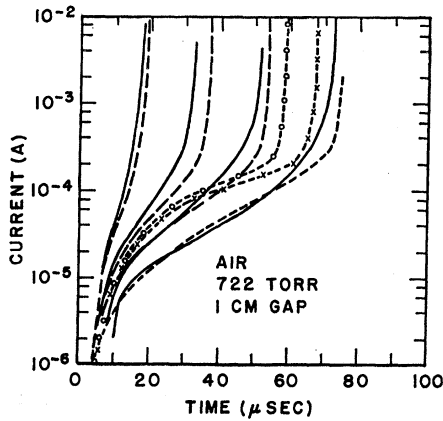
FIG. 2. Comparison between measured[3] (solid curves) and cal-
culated current-growth versus time curves. Long-dashed curves
used 90% γ_p, short-dashed curve 80% γ_p and curves with indi-
vidual points, 100% γ_p. The curve with crosses used $\mu_- p = 2 \times 10^5$
cm^2/V sec and the curve with open points used a photon delay,
$\tau = 1 \times 10^{-7}$ sec. The overvoltage used in each case may be ob-
tained from Figs. 3 and 4.

should be compared. The most critical criterion is the
agreement between the slopes (growth constants) of the
curves in the region of exponential growth, before
space-charge distortion and after the initial growth
phase, for a given formative time lag. It is seen that the
two curves with 100% γ_p have growth constants which
are much smaller than those of the measured curves for
the appropriate breakdown times. The curves for which
γ_i components were used agree with the measured curves
well within the experimental scatter.[3]

A second criterion for comparison of the various
curves is the separation of the curves at the "shoulder,"
i.e., at $\sim 10^{-5}$ A. It is seen that the calculations using
a γ_i component do show the proper separation while the
others do not. Curves calculated assuming 100% γ_p
are not shown in Fig. 2 for smaller formative time lags
since the figure would lose clarity. For breakdown times
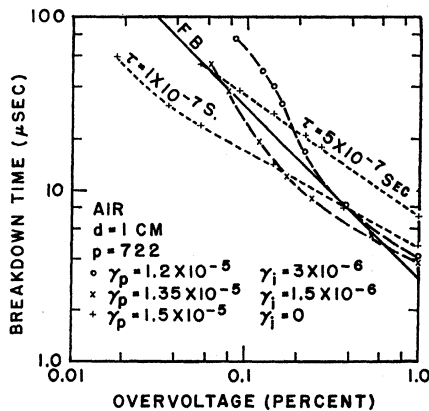of less than ~ 30 μsec, the curves using 100% γ_p are

FIG. 3. Plot of calculated (points) breakdown times as a function
of overvoltage. The solid line is the reference line from the meas-
ured data of Fisher and Bederson (Ref. 2) as given in Fig. 1.

nearly equal to the others in agreement with the meas-
ured curves.

An area of 20 cm^2 was used for all of these calcula-
tions. This is roughly half the experimental cathode area
and agrees well with the value of 22.9 cm^2 used by
Köhrmann.[6] At the current of $\sim 3 \times 10^{-4}$ A, sharper
breaks are observed in the two longer calculated break-
down-time curves than in the corresponding measured
curve. This can probably be explained by the contrac-
tion of the discharge due to space-charge effects.

The above calculations were made with $J_0 = 5 \times 10^{-13}$
A/cm^2, $R = 1 \times 10^4$ Ω, $C = 1 \times 10^{-10}$ F, $V(0) = 26.5$ kV,
and various step voltages applied at $t = 0$. These values
are generally consistent with those used by Bandel and
by FB and the effect of their variation is presented
below. Most calculations were made with $R = 1 \times 10^4$ Ω
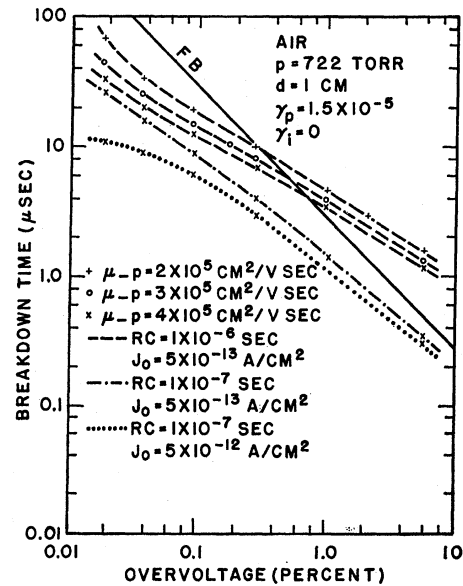rather than the $\sim 1 \times 10^3$ Ω used by FB and Bandel,

FIG. 4. Effects of variations of electron mobility, external illu-
mination and external circuit RC time constants upon 100% γ_p
calculations. The solid curve is again from Fig. 1.

since it is believed that the calculated collapse of
voltage upon breakdown is more accurate in this case.
It is shown below that the RC time constant is relatively
unimportant for the longer time lags.

A plot of the breakdown times as a function of per-
cent overvoltage for all but one of the above calcula-
tions is given in Fig. 3, which also includes many
additional calculations. The reference curve from Fig. 1,
based on FB's[2] measurements, is also included in Fig. 3.
It is seen that in calculations assuming 100% γ_p, no
one value of photon delay can be used to obtain agree-
ment with the measured data. The 90% γ_p curve is
well within the experimental scatter of the measured
curves.

A second plot of calculated breakdown times as a
function of percent overvoltage is given in Fig. 4.

These calculations all assume 100% γ_p and show the effect of varying electron mobilities. Again the characteristic measured curve from Fig. 1 shows that agreement is not obtained with the 100% γ_p calculations. Also shown in Fig. 4 is the effect of changing J_0 and the circuit RC time constant.

All of the above calculations were made with a constant approach voltage, $V(0) = 26.5$ kV. A sequence of calculations was also made for which the approach voltages were either 1 or 2 kV below the final applied voltages. The results are shown in Fig. 5 for 80% γ_p. Also shown are further results of varying J_0 and RC. It is noted that the variation of J_0 is unimportant at higher overvoltages ($>1\%$) but is increasingly important at lower overvoltages. The values of overvoltages have not been corrected for the lowering of the breakdown voltage due to external illumination. The calculations also show that FB[2] could not be expected to have noted the effects of either changing the approach voltage or the external illumination in their experiments, considering their scatter of data.
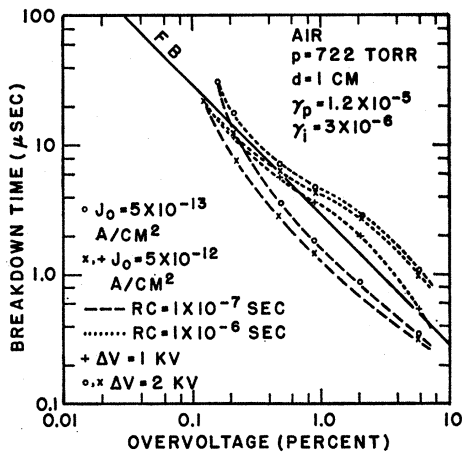

FIG. 5. Effects of variations of approach voltage, external illumination and external circuit RC time constants upon 80% γ_p calculations. The solid curve is again from Fig. 1.

For large overvoltages there is little difference in time lags as a function of the ratio of γ_i to γ_p. For time lags of the order of 10 μsec ($\sim\frac{1}{2}$ ion transit time) considerable difference begins to appear. This is mainly due to the small reduction of γ_p in those calculations including a γ_i component. This is equivalent to a small shift in overvoltage, but is completely independent of the accuracy to which γ values are known. Calculations made with total γ values changed by an order of magnitude give nearly identical time lag versus overvoltage curves.

An interesting effect is noted in Fig. 6 in which the individual components of the total current are plotted as a function of time. It is noted that there is a definite change of the growth rate of the electron current at one ion transit time (~17 μsec). No change is noted in either the ion current or in the total current.
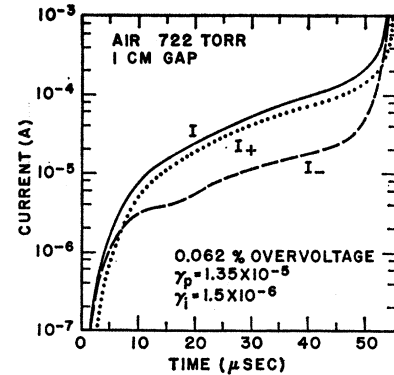

FIG. 6. Electron current I_-, positive ion current I_+, and total current I as a function of time, showing change of growth rate of I_- at one ion transit time.

As a check on the effect of the initial conditions assumed for calculations, some calculations were made with no initial charge carriers in the gap at $t = 0$ except for one electron/cm^2 emitted from the cathode. The results are shown as dashed curves in Fig. 7 and may be compared with the solid line curves, which were calculated with the previously mentioned equilibrium distribution of charges as initial conditions. Although there are two orders of magnitude difference in current at $t = 0$, the total currents are sensibly equal within a few electron transit times. The ion-current densities differ by only about 10% at 0.5 μsec, only $\sim1/34$ of an ion transit time; however, the distribution of ions in the cathode region is entirely different. Breakdown times, determined graphically, are identical. This example shows why only small effects of initial conditions have been noted in experiments.

All of the preceding calculations have been made with only 20 calculation intervals across the gap ($M = 20$). A few calculations have been made with $M = 40$, which reduces the error in breakdown voltage from 3.82 to 1.97%. Unexpectedly, the more accurate calculations reduced the breakdown time by about 5 to 10% for overvoltages above 0.5%. Earlier estimates[13], based on equilibrium current-growth rates, led to the expectation of longer breakdown times and the consequent estimate
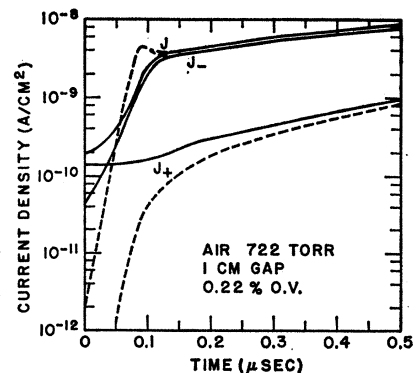

FIG. 7. Electron (J_-), Ion (J_+) and total (J) current density as a function of time. Solid curves are for an equilibrium distribution of charges in the gap. Dashed curves pertain to calculations made with one electron/cm^2 emitted from the cathode at $t = 0$.

[13] A. L. Ward, Proceedings of the Sixth International Conference on Ionization Phenomena in Gases, edited by P. Hubert (SERMA, Paris, 1963) Vol. II, p. 313.
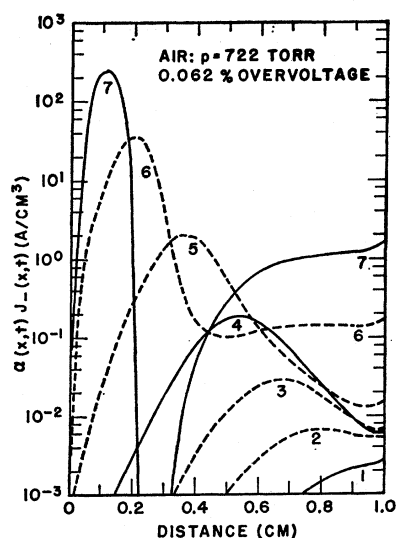
FIG. 8. Plot of the ionization rate as a function of distance across the gap at various times in μsec and current densities in mA/cm², respectively, as follows: (1) 53.89, 0.130, (2) 54.10, 0.53, (3) 54.18, 2.18, (4) 54.22, 9.85, (5) 54.243, 42.95, (6) 54.252, 193.9 and (7) 54.255, 469.8.

that smaller ion portions of the secondary coefficient would be required as the number of calculation intervals increased. Doubling M roughly quadruples the computation time, thus making calculations with larger M values at very low overvoltages too costly. It is felt that the present error, due to using a small number of calculation intervals, is well within the scatter of experimental data. Doubling M also cuts the diffusion coefficient in half according to Eq. (9). The small effect of this reduction on the results strongly indicates that the error in the calculated diffusion current is not important.

Bandel[3] stated that spark breakdown occurred within 1 μsec after the end of his recorded current growth curves. Some of the present calculations have been extended to much higher currents than shown in Fig. 2. The distribution of light intensity across the gap as a function of time has been measured by a number of experimenters during the final stages of breakdown. Assuming the equality of the ionization and excitation coefficients, the quantity $\alpha(x,t)j_-(x,t)$ should be proportional to the light intensity. A plot of αj_- as a function of distance at various times is shown in Fig. 8. The calculation was made assuming 90% γ_p and 0.062% overvoltage. The current growth at earlier times is shown in Fig. 2

as the curve with a breakdown time of $\sim$54.2 μsec. Curves similar to Fig. 8, but for 80% γ_p, 0.22% overvoltage, and a breakdown time of $\sim$11.5 μsec, have been published previously.[13] Comparison of the two sets of curves show that this final stage of breakdown is nearly independent of overvoltage. In fact, when αj_- values for the various x values are plotted as a function of $J(t)$ for the two cases, the curves nearly coincide. A plot of the positions of the maxima of the αj_- curves as a function of time show that the maximum moves from the anode with an increasing velocity, reaching 3×10^7 cm sec^{-1} near the cathode. This is the same order of magnitude as that measured for the propagating light front in planar breakdown.

V. CONCLUSIONS

It has been shown that Bandel's measured current-growth curves and FB's breakdown time as a function of overvoltage curves may be fitted satisfactorily with calculations which include a 10% ion portion in the total secondary coefficient. A poorer fit in both cases is obtained if a 100% photon secondary coefficient is used with either a delayed photon simulation or a lower electron mobility to simulate an attachment-detachment process. Better experimental data for formative time lags of greater than an ion transit time will be needed to resolve this question.

Calculations have shown the effect upon the breakdown time of varying the approach voltage, the external illumination, and the RC time constant of the external circuit. These calculations are in qualitative agreement with experimental results, but a reduction in the scatter of the experimental data is needed for a good quantitative check. Lastly, the calculations indicate that a light front propagates from the anode toward the cathode with a velocity increasing up to 3×10^7 cm sec^{-1}, largely independent of overvoltage. This is in qualitative agreement with observations.

It has been shown that the Townsend avalanche mechanism, including space charge, is adequate to explain the entire breakdown transition for low overvoltages in air at near-atmospheric pressure. Results of calculations for another gas at high overvoltages have been submitted for publication.